

## An Effect of Barrier Shapes for Reducing a Peak Overpressure around a Hydrogen Energy Facility

Hyung Seok Kang, Sang Min Kim, Jongtae Kim, and Keun Sang Choi  
KAERI, 111, Daedeok-daero, 989 Beon-gil, Yuseong-Gu, Daejeon, 34057, Republic of Korea  
\*Corresponding author: hskang3@kaeri.re.kr

### 1. Introduction

An installation of a barrier with various shapes at a hydrogen refueling station (HFS) is being considered to reduce a safety distance between a HFS and a protection facility, which is required by Korea Gas Safety Codes [1-3]. The safety distance may be determined on the basis of a peak overpressure limit according to the class of the protection facility [4,5]. We established a reasonable CFD analysis methodology with an error range of approximately 30% for predicting a peak overpressure variation from a hydrogen explosion region to a blast wave region on the basis of Stanford Research institute (SRI) Test No. 4-02 [6,7]. In this study, an evaluation for a rectangular barrier with height 4 m was performed by using the established CFD analysis methodology to see an effect of barrier shapes in the peak overpressure reduction on the basis of SRI Test No. 4-02.

### 2. Hydrogen Explosion Tests with the Barrier

SRI performed a hydrogen explosion test using a hydrogen-air mixture volume  $5.2 \text{ m}^3$  with the stoichiometric condition in an open space by varying the ignition method and the barrier existence like as Fig. 1 [7]. A plate type barrier with height 2 m, wide 10 m, and thickness 0.1 m was located at 4 m from the right boundary of the tent where the hydrogen-air mixture was located. They measured the peak overpressure at 11 m, 21 m and 41 m from the tent as well as the peak overpressure at 2 m behind and front the barrier, respectively, such as P2 and P4 (Fig. 1). In Tests 4-02 and 5-02, the overpressure at 11 m from the ignition point was reduced to approximately 30 – 40 % of the overpressure measured in Tests 4-01 and 6-01 without the barrier (Fig. 2). However, the overpressures at 41 m did not show the difference resulted from the barrier existence.

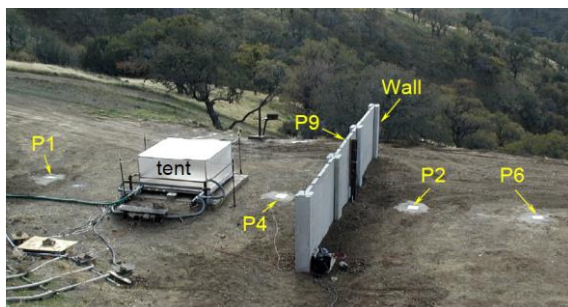


Fig. 1. SRI Facility [7]

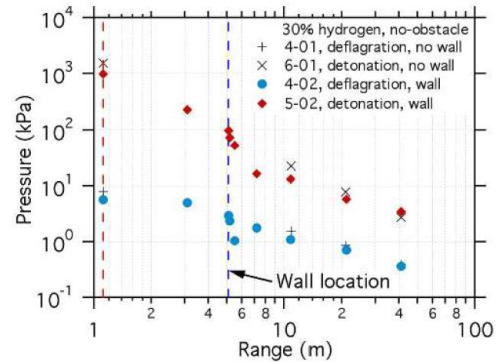
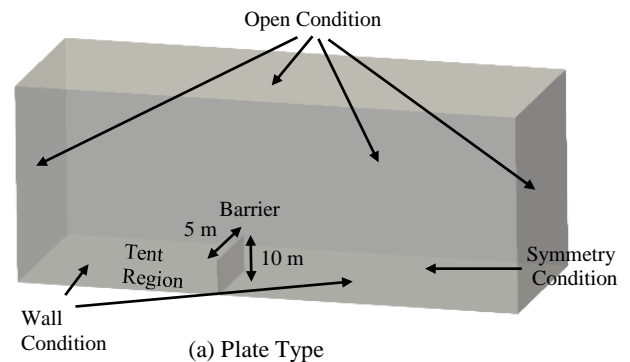


Fig. 2. Peak Overpressures in the SRI Tests [7]

### 3. CFD Analysis

#### 3.1 Grid Model and Flow Field Models

A 3-dimensional and half symmetric grid model (Fig. 3(a), Table 1) for simulating the tent, plate type barrier, and air environment region to 21 m from the ignition point was generated on basis of the test facility and the safety distance regulation by using the blockMesh utility in OpenFOAM-v1912 [8]. A rectangular barrier with height 4 m was located at the same location as the plate barrier in the grid model, and also its distance from the tent boundary in y-direction was assumed as 4 m, which is similar to that of distance in x-direction. A total of 3,029,280 hexahedral mesh cells for the grid model with the plate type barrier was produced. As for the rectangular type barrier, 3,185,705 cells were generated in the grid model (Fig. 3(b)). A dense mesh cell distribution with an approximately 2 cm cell length was located in the tent region ( $2.2 \text{ m} \times 1.1 \text{ m} \times 1.07 \text{ m}$ ) to resolve a rapid flame propagation due to the turbulence generation [9]. A symmetric condition was applied along the half cut surface in the grid model. An open condition was given to all the surrounding surfaces except for the bottom and half-cut surface. A wall condition was given to the surfaces of the barrier and the bottom of the grid model.



(a) Plate Type

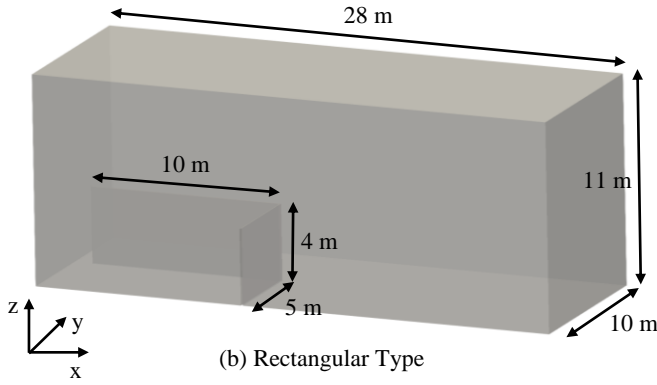


Fig. 3. Grid Model for Barrier Shapes

Table 1: Initial conditions according to Barrier Shapes

Test No.	H <sub>2</sub> -Air Volume	H <sub>2</sub> Con. (Vol. %)	Barrier Height	Barrier Shape
Case-1	5.2 m <sup>3</sup>	29.9	2 m	Plate
Case-2	5.2 m <sup>3</sup>	29.9	4 m	Rectangular

To analyze the rapid flame propagation in the tent region, the modified XiFoam solver was used together with other governing equations of the mass conservation, Navier-Stokes momentum, total energy, turbulence under the pimple solver algorithm in OpenFOAM-v1912 [8,10]. The spark ignition model representing the pressure, temperature, and volume of the activated region [9] was used for simulating the ignition energy 40 J provided by the electric spark device in the test. The time step size used in the transient calculation of 0.11 s was approximately 0.001 to 0.1 ms for obtaining converged solutions.

### 3.2 Discussion on the CFD Analysis Results

The CFD analysis results for the pressure distribution on the barrier surfaces and pressure wave propagation to the environment at 0.036 s are shown in Fig. 4. According to Fig. 4(a), the pressure wave from the tent region bypasses the plate barrier with height 2 m after passing the inner surface of the barrier in y-direction, and continually propagates to the air environment. However, in case of the rectangular barrier with height 4 m, most of the pressure wave propagating along the horizontal direction from the tent region reflects to the ground or the air environment with the reduced magnitude after colliding with the barrier. As the results of this pressure wave propagation patterns according to the barrier shapes, the peak overpressure at P2, which locates at the rear region of the barrier, under the rectangular barrier decreases to approximately 79.3% of that of the plate barrier like as “A” in Fig. 5(a). The peak overpressure at P4, which locates the front of the barrier, under the rectangular barrier increases 30% when compared to that of the plate barrier (Fig. 5(b), “B”). Figure 6 shows the density distribution of the air and the mixture gas according to the time pass, which is resulted from the pressure wave propagation in the air environment.

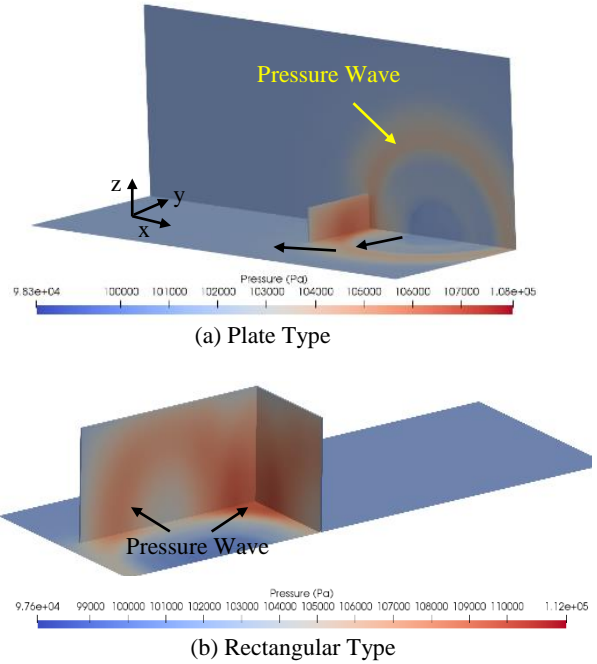


Fig. 4. Pressure Distribution on Barrier Surfaces

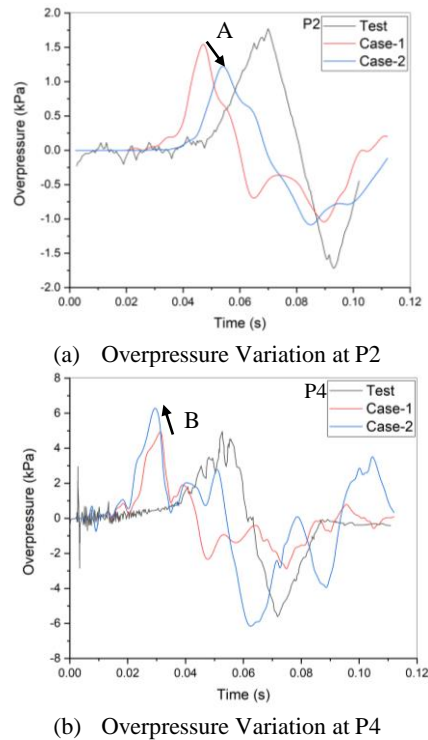
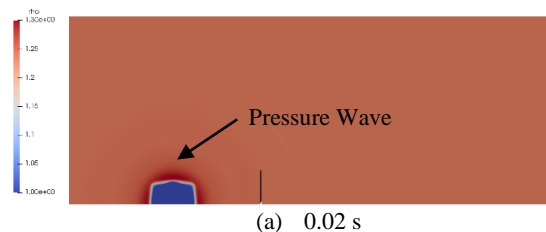


Fig. 5. Comparison of Pressure Behaviors at P2 and P4 between Test Data, Case-1, and Case-2



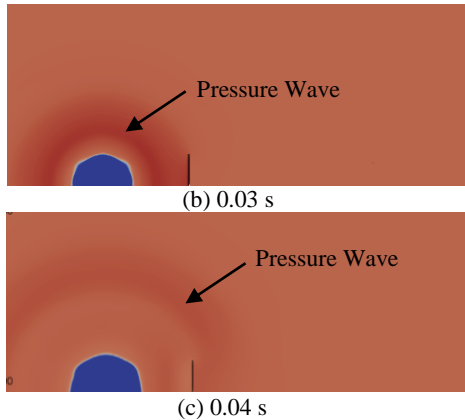


Fig. 6. Density Distribution as Time Passes

Table 2: Calculated Peak Overpressures by OpenFOAM

Test No.	P3 [kPa]	(P4-P2) / P3	P6 [kPa] (11m)	P7 [kPa] (21m)
Case-1	8.876	0.381	1.116	0.578
Case-2	9.369	0.540	1.018	0.556

In order to estimate the performance depending on the barrier type to reduce the peak overpressure, we introduce the normalized peak overpressure difference between P4 and P2 divided by the peak overpressure at P3 locating in the tent because the peak overpressure in the tent varies due to the reflection effect when the rectangular barrier is used. According to the barrier performance parameter in Table 2, the peak overpressure reduction rate by the rectangular barrier is increased to approximately 50% when compared to the plate barrier. In addition, the overpressures at the far field of 11 m and 21 m from the ignition point under the rectangular barrier are also decreased to approximately 90% those of the plate barrier (Table 2).

#### 4. Conclusions and Further Work

We evaluated a rectangular barrier with height 4 m by using the established CFD analysis methodology with an error range of approximately 30% to see its performance of a peak overpressure reduction on the basis of SRI Test No. 4-02. Through the CFD analysis using the modified XiFoam in OpenFoam-v1912, we found that the rectangular barrier increased the peak overpressure reduction rate as approximately 50% when compared to the plate barrier. It is therefore thought that the rectangular shape is a more useful geometry configuration for the barrier around the hydrogen energy facility to reduce the peak overpressure than the plate shape. However, this numerical result should be validated through the comparison with experimental results, and also the pressure wave effect on the barrier structure will also be examined by the Fast Fourier Transform (FFT) analysis.

#### ACKNOWLEDGMENTS

This work was supported by the Korea Institute of Energy Technology Evaluation and Planning (KETEP) grant funded by the Korea government (Ministry of Trade, Industry and Energy) (No. 20215810100020).

#### REFERENCES

- [1] K. S. Kim, Development of Design Technology and Safety Standard in the Protection Wall for Blast Mitigations in Hydrogen Station, Research Plan Report, No. 20215810100020, KGS, 2021.
- [2] KGS, Facility/Technical/Inspection Code for Fuel Vehicles Refueling by Type of On-Site Hydrogen Production, Technical Standards, KGS FP216, 2020.
- [3] KGS, Facility/Technical/Inspection Code for Fuel Vehicles Refueling by Type of Compressed Hydrogen Delivery, Technical Standards, KGS FP217, 2020.
- [4] H. S. Kang, S. B. Kim, M. H. Kim, W.-J. Lee, H. C. NO "Regulatory Issues on the Safety Distance between a VHTR and a H<sub>2</sub> Production Facility and an Overpressure Prediction Using Correlations and a CFD Analysis for the JAEA Explosion Test in an Open Space", *NT*, Vol. 166, pp. 86-100, 2009.
- [5] Korea Occupational Safety and Health Agency, Estimating Methodology for Accident Damage, CODE No. P-31-2001, 2001.
- [6] H. S. Kang, S. M. Kim, and J. Kim, "An Effect of a Barrier for Reducing a Safety Distance around a Hydrogen Energy Facility", *Proceeding of KNS Spring Meeting*, Jeju, Korea, May 19-20, 2022.
- [7] Mark A. Groethe and James D. Colton, FY02 Annual Report on Hydrogen Safety in the World Energy Network, Technical Report, Project 10367, SRI, 2003.
- [8] OpenFOAM-v1912, <https://www.openfoam.com>
- [9] H. S. Kang, H. C. NO, S. B. Kim, and M. H. Kim, "Methodology of CFD Analysis for Evaluating H<sub>2</sub> Explosion Accidents in an Open Space", *IJHE*, Vol. 40, pp. 3075-3090, 2015.
- [10] S. M. Kim, H. S. Kang, and J. Kim, Validation of Combustion Models for Analysis of Hydrogen Burn in a Containment, Technical Report, KAER/TR-8517/2020, KAERI, 2020.